

Search For the Decay $B \rightarrow D_{s1}^+(2536)X$

CLEO Collaboration

(August 14, 2018)

Abstract

We have searched for the decay $B \rightarrow D_{s1}^+(2536)X$ and measured an upper limit for the inclusive branching fraction of $\mathcal{B}(B \rightarrow D_{s1}^+X) < 0.95\%$ at the 90% confidence level. This limit is small compared with the total expected $B \rightarrow \bar{D}^{(*)}D^{(*)}KX$ rate. Assuming factorization, the D_{s1}^+ decay constant is constrained to be $f_{D_{s1}^+} < 114$ MeV at the 90% confidence level, at least 2.5 times smaller than that of D_s^+ .

PACS numbers: 13.25.Hw, 14.40.Nd

M. Bishai,¹ J. Fast,¹ J. W. Hinson,¹ N. Menon,¹ D. H. Miller,¹ E. I. Shibata,¹
 I. P. J. Shipsey,¹ M. Yurko,¹ S. Glenn,² S. D. Johnson,² Y. Kwon,^{2,*} S. Roberts,²
 E. H. Thorndike,² C. P. Jessop,³ K. Lingel,³ H. Marsiske,³ M. L. Perl,³ V. Savinov,³
 D. Ugolini,³ R. Wang,³ X. Zhou,³ T. E. Coan,⁴ V. Fadeyev,⁴ I. Korolkov,⁴ Y. Maravin,⁴
 I. Narsky,⁴ V. Shelkov,⁴ J. Staeck,⁴ R. Stroynowski,⁴ I. Volobouev,⁴ J. Ye,⁴ M. Artuso,⁵
 F. Azfar,⁵ A. Efimov,⁵ M. Goldberg,⁵ D. He,⁵ S. Kopp,⁵ G. C. Moneti,⁵ R. Mountain,⁵
 S. Schuh,⁵ T. Skwarnicki,⁵ S. Stone,⁵ G. Viehhauser,⁵ X. Xing,⁵ J. Bartelt,⁶ S. E. Csorna,⁶
 V. Jain,^{6,†} K. W. McLean,⁶ S. Marka,⁶ R. Godang,⁷ K. Kinoshita,⁷ I. C. Lai,⁷
 P. Pomianowski,⁷ S. Schrenk,⁷ G. Bonvicini,⁸ D. Cinabro,⁸ R. Greene,⁸ L. P. Perera,⁸
 G. J. Zhou,⁸ B. Barish,⁹ M. Chadha,⁹ S. Chan,⁹ G. Eigen,⁹ J. S. Miller,⁹ C. O'Grady,⁹
 M. Schmidtler,⁹ J. Urheim,⁹ A. J. Weinstein,⁹ F. Würthwein,⁹ D. W. Bliss,¹⁰ G. Masek,¹⁰
 H. P. Paar,¹⁰ S. Prell,¹⁰ V. Sharma,¹⁰ D. M. Asner,¹¹ J. Gronberg,¹¹ T. S. Hill,¹¹
 D. J. Lange,¹¹ R. J. Morrison,¹¹ H. N. Nelson,¹¹ T. K. Nelson,¹¹ J. D. Richman,¹¹
 D. Roberts,¹¹ A. Ryd,¹¹ M. S. Witherell,¹¹ R. Balest,¹² B. H. Behrens,¹² W. T. Ford,¹²
 H. Park,¹² J. Roy,¹² J. G. Smith,¹² J. P. Alexander,¹³ C. Bebek,¹³ B. E. Berger,¹³
 K. Berkelman,¹³ K. Bloom,¹³ V. Boisvert,¹³ D. G. Cassel,¹³ H. A. Cho,¹³ D. S. Crowcroft,¹³
 M. Dickson,¹³ S. von Dombrowski,¹³ P. S. Drell,¹³ K. M. Ecklund,¹³ R. Ehrlich,¹³
 A. D. Foland,¹³ P. Gaidarev,¹³ L. Gibbons,¹³ B. Gittelman,¹³ S. W. Gray,¹³ D. L. Hartill,¹³
 B. K. Heltsley,¹³ P. I. Hopman,¹³ J. Kandaswamy,¹³ P. C. Kim,¹³ D. L. Kreinick,¹³
 T. Lee,¹³ Y. Liu,¹³ N. B. Mistry,¹³ C. R. Ng,¹³ E. Nordberg,¹³ M. Ogg,^{13,‡}
 J. R. Patterson,¹³ D. Peterson,¹³ D. Riley,¹³ A. Soffer,¹³ B. Valant-Spaight,¹³ C. Ward,¹³
 M. Athanas,¹⁴ P. Avery,¹⁴ C. D. Jones,¹⁴ M. Lohner,¹⁴ C. Prescott,¹⁴ J. Yelton,¹⁴
 J. Zheng,¹⁴ G. Brandenburg,¹⁵ R. A. Briere,¹⁵ A. Ershov,¹⁵ Y. S. Gao,¹⁵ D. Y.-J. Kim,¹⁵
 R. Wilson,¹⁵ H. Yamamoto,¹⁵ T. E. Browder,¹⁶ Y. Li,¹⁶ J. L. Rodriguez,¹⁶ T. Bergfeld,¹⁷
 B. I. Eisenstein,¹⁷ J. Ernst,¹⁷ G. E. Gladding,¹⁷ G. D. Gollin,¹⁷ R. M. Hans,¹⁷ E. Johnson,¹⁷
 I. Karliner,¹⁷ M. A. Marsh,¹⁷ M. Palmer,¹⁷ M. Selen,¹⁷ J. J. Thaler,¹⁷ K. W. Edwards,¹⁸
 A. Bellerive,¹⁹ R. Janicek,¹⁹ D. B. MacFarlane,¹⁹ P. M. Patel,¹⁹ A. J. Sadoff,²⁰ R. Ammar,²¹
 P. Baringer,²¹ A. Bean,²¹ D. Besson,²¹ D. Coppage,²¹ C. Darling,²¹ R. Davis,²¹ S. Kotov,²¹
 I. Kravchenko,²¹ N. Kwak,²¹ L. Zhou,²¹ S. Anderson,²² Y. Kubota,²² S. J. Lee,²²
 J. J. O'Neill,²² S. Patton,²² R. Poling,²² T. Riehle,²² A. Smith,²² M. S. Alam,²³
 S. B. Athar,²³ Z. Ling,²³ A. H. Mahmood,²³ H. Severini,²³ S. Timm,²³ F. Wappler,²³
 A. Anastassov,²⁴ J. E. Duboscq,²⁴ D. Fujino,^{24,§} K. K. Gan,²⁴ T. Hart,²⁴ K. Honscheid,²⁴
 H. Kagan,²⁴ R. Kass,²⁴ J. Lee,²⁴ M. B. Spencer,²⁴ M. Sung,²⁴ A. Undrus,^{24,**} R. Wanke,²⁴
 A. Wolf,²⁴ M. M. Zoeller,²⁴ B. Nematy,²⁵ S. J. Richichi,²⁵ W. R. Ross,²⁵ and P. Skubic²⁵

*Permanent address: Yonsei University, Seoul 120-749, Korea.

†Permanent address: Brookhaven National Laboratory, Upton, NY 11973.

‡Permanent address: University of Texas, Austin TX 78712

§Permanent address: Lawrence Livermore National Laboratory, Livermore, CA 94551.

**Permanent address: BINP, RU-630090 Novosibirsk, Russia.

- ¹Purdue University, West Lafayette, Indiana 47907
- ²University of Rochester, Rochester, New York 14627
- ³Stanford Linear Accelerator Center, Stanford University, Stanford, California 94309
- ⁴Southern Methodist University, Dallas, Texas 75275
- ⁵Syracuse University, Syracuse, New York 13244
- ⁶Vanderbilt University, Nashville, Tennessee 37235
- ⁷Virginia Polytechnic Institute and State University, Blacksburg, Virginia 24061
- ⁸Wayne State University, Detroit, Michigan 48202
- ⁹California Institute of Technology, Pasadena, California 91125
- ¹⁰University of California, San Diego, La Jolla, California 92093
- ¹¹University of California, Santa Barbara, California 93106
- ¹²University of Colorado, Boulder, Colorado 80309-0390
- ¹³Cornell University, Ithaca, New York 14853
- ¹⁴University of Florida, Gainesville, Florida 32611
- ¹⁵Harvard University, Cambridge, Massachusetts 02138
- ¹⁶University of Hawaii at Manoa, Honolulu, Hawaii 96822
- ¹⁷University of Illinois, Urbana-Champaign, Illinois 61801
- ¹⁸Carleton University, Ottawa, Ontario, Canada K1S 5B6
and the Institute of Particle Physics, Canada
- ¹⁹McGill University, Montréal, Québec, Canada H3A 2T8
and the Institute of Particle Physics, Canada
- ²⁰Ithaca College, Ithaca, New York 14850
- ²¹University of Kansas, Lawrence, Kansas 66045
- ²²University of Minnesota, Minneapolis, Minnesota 55455
- ²³State University of New York at Albany, Albany, New York 12222
- ²⁴Ohio State University, Columbus, Ohio 43210
- ²⁵University of Oklahoma, Norman, Oklahoma 73019

I. INTRODUCTION

One of the outstanding issues in B meson physics is the semileptonic branching fraction puzzle. Experimentally $\mathcal{B}(B \rightarrow X\ell\nu)$ is measured to be $(10.43 \pm 0.24)\%$ [1], whereas theoretical calculations have difficulties accommodating a branching fraction below $\sim 12.5\%$ [2]. One way to reduce the theoretical expectations is through a two-fold enhancement in the assumed $\bar{b} \rightarrow \bar{c}c\bar{s}$ rate [3], which is estimated to be $\sim 15\%$ from the measured inclusive rates for $B \rightarrow D_s^+ X$ and $B \rightarrow \psi X$.

Recently, Buchalla *et al.* [4] and Blok *et al.* [5] have suggested that a significant fraction of the $\bar{b} \rightarrow \bar{c}c\bar{s}$ transition hadronizes into $B \rightarrow \bar{D}DKX$. This is supported by CLEO's [6] observation of “wrong-sign” D mesons from B decays, $\mathcal{B}(B \rightarrow DX) = (7.9 \pm 2.2)\%$, where the D comes from the virtual $W^+ \rightarrow c\bar{s}$. The ALEPH [7] and DELPHI [8] collaborations have also observed sizeable $B \rightarrow D^{(*)}\bar{D}^{(*)}X$ decay rates. Exclusive B decays involving wrong-sign D mesons can result from (1) resonant $B \rightarrow \bar{D}^{(*)}D_s^{**}$ decays, where the $W^+ \rightarrow c\bar{s}$ hadronizes to an excited D_s^+ meson that decays into DKX ; and (2) non-resonant $B \rightarrow \bar{D}^{(*)}D^{(*)}K$ decays. This paper explores one possibility in the first case, namely, the decays $B \rightarrow D_{s1}^+(2536)X$ where D_{s1}^+ is the narrow P-wave D_s^+ meson with $J^P = 1^+$. The “upper-vertex” production of D_{s1}^+ from $W^+ \rightarrow c\bar{s}$ hadronization is shown in Figure 1(a). In addition, D_{s1}^+ mesons can be produced from “lower-vertex” decays $b \rightarrow \bar{c}ud$ with the creation of an $s\bar{s}$ quark pair, as shown in Figure 1(b). This produces right-sign D mesons; however, the decay rate is expected to be small. Throughout this paper charge conjugate states are implied.

Continuum D_{s1}^+ production has been thoroughly studied [1]. The D_{s1}^+ is just above the D^*K mass threshold and decays dominantly into $D^{*0}K^+$ and $D^{*+}K^0$. Other possible decay channels are negligible: $D_s^{(*)+}\pi^0$ due to isospin conservation, $D_s^{(*)+}(n\pi)$ due to OZI suppression [9], DK or $D_s^+\pi^0$ due to angular momentum and parity conservation, and $D_s^{(*)+}\gamma$ due to the small radiative decay rate.

II. DATA SAMPLE AND EVENT SELECTION

The data used in this analysis were selected from hadronic events collected by the CLEO II detector at the Cornell Electron Storage Ring (CESR). The CLEO II detector [10] is a large solenoidal detector with 67 tracking layers and a CsI electromagnetic calorimeter that provides efficient π^0 reconstruction. The data consist of an integrated luminosity of 3.11 fb^{-1} at the $\Upsilon(4S)$ resonance, corresponding to 3.3×10^6 $B\bar{B}$ events. To evaluate non- $B\bar{B}$ backgrounds we also collected 1.61 fb^{-1} of “continuum” data 60 MeV below the $\Upsilon(4S)$ resonance.

The inclusive $B \rightarrow D_{s1}^+ X$ decay is studied by reconstructing the decay channels $D_{s1}^+ \rightarrow D^{*0}K^+$ and $D_{s1}^+ \rightarrow D^{*+}K_s^0$ using the decay modes $D^{*0} \rightarrow D^0\pi^0$ and $D^{*+} \rightarrow D^0\pi^+$. The D^0 is reconstructed using the decay modes $D^0 \rightarrow K^-\pi^+$ and $K^-\pi^+\pi^0$. Hadronic events are required to satisfy the ratio of Fox-Wolfram moments [11] $R_2 = H_2/H_0 < 0.3$ to reduce the background from continuum events.

Charged tracks, except pions from K_s^0 decays, are required to be consistent with coming from the primary interaction point. Charged kaon and pion candidates are identified using specific ionization (dE/dx) and, when available, time-of-flight (TOF) information. For kaon

identification, we consider the relative probability for a charged track to be a kaon, $\mathcal{R}_K = \mathcal{P}_K/(\mathcal{P}_\pi + \mathcal{P}_K + \mathcal{P}_p)$, where \mathcal{P} is the χ^2 probability for a given particle hypothesis. The requirement on \mathcal{R}_K depends on the decay mode of interest. Pion candidates are identified by requiring the dE/dx and, when available, TOF information to be within 3 standard deviations (σ) of that expected for pions. We select K_S^0 candidates through the decay to $\pi^+\pi^-$ by requiring a decay vertex displaced from the primary interaction point and a K_S^0 invariant mass within 10 MeV/c² of its nominal value. We reconstruct π^0 candidates through the decay to $\gamma\gamma$ by requiring candidates to have an invariant mass within 2.5 standard deviations ($\sigma \approx 5$ MeV/c²) of the nominal π^0 mass.

The $K^-\pi^+$ and $K^-\pi^+\pi^0$ combinations are required to have a kaon identification of $\mathcal{R}_K > 0.5$ and 0.7, respectively, and an invariant mass within 15 and 25 MeV/c² ($\sim 2\sigma$) of the nominal D^0 mass, respectively. In addition, we select regions of the $D^0 \rightarrow K^-\pi^+\pi^0$ Dalitz plot to take advantage of the known resonant substructure [12]. For the $D_{s1}^+ \rightarrow D^{*0}K^+$ mode, the Dalitz cut reduces the signal efficiency by 40% and the background by 80%. We relax the Dalitz cut for the $D^{*+}K_S^0$ mode since the combinatoric background is substantially lower.

The $D^{*+} \rightarrow D^0\pi^+$ candidates are required to have a mass difference $M(D^0\pi^+) - M(D^0)$ within 1.5 MeV/c² ($\sim 2\sigma$) of the nominal value of 145.4 MeV/c², where $M(X)$ is the reconstructed invariant mass of X . Similarly, the $D^{*0} \rightarrow D^0\pi^0$ candidates are required to have a mass difference $M(D^0\pi^0) - M(D^0)$ within 1.5 MeV/c² ($\sim 2\sigma$) of the nominal value of 142.1 MeV/c². To form D_{s1}^+ candidates charged kaons are combined with D^{*0} candidates and K_S^0 's are combined with D^{*+} candidates. Since the primary kaons from $D_{s1}^+ \rightarrow D^{*0}K^+$ decays have low momentum, we can impose a stringent $\mathcal{R}_K > 0.9$ requirement on the K^+ with negligible loss of efficiency. The D_{s1}^+ candidates are required to have a scaled momentum $x_p = p_{D_{s1}^+}/\sqrt{E_{beam}^2 - M_{D_{s1}^+}^2} < 0.45$, which is the kinematic limit for $B \rightarrow D_{s1}^+X$ decays. (We ignore the negligible contributions from $b \rightarrow u$ decays.) Upper-vertex D_{s1}^+ production results in a maximum x_p of 0.35, and this requirement is imposed when determining the D_{s1}^+ decay constant. The D_{s1}^+ decay channels with π^0 's in the final state often have multiple D_{s1}^+ candidates per event. We select the candidate with the highest χ^2 probability of being a D_{s1}^+ , which is derived from the invariant masses of the reconstructed π^0 , D^0 and D^* mesons.

III. RAW YIELDS

The D_{s1}^+ signal is identified using the D^*K mass difference, $\Delta M_1 = M(D^{*0}K^+) - M(D^{*0}) - M_{K^+}$ and $\Delta M_2 = M(D^{*+}K_S^0) - M(D^{*+}) - M_{K_S^0}$, where M_{K^+} and $M_{K_S^0}$ are the known masses [1]. The D^*K mass difference signal has a resolution that is two to four times smaller than the corresponding signal in the reconstructed D^*K invariant mass distribution. The ΔM_1 and ΔM_2 distributions are shown in Figure 2, where the $D^0 \rightarrow K^-\pi^+$ and $K^-\pi^+\pi^0$ modes have been added together. The data is fit with a Gaussian signal and a threshold background function. The Gaussian width is fixed to that expected from a GEANT-based Monte Carlo simulation [13] ($\sigma = 2.4 - 3.6$ MeV/c², depending on the mode) and the mean is fixed to the measured D_{s1}^+ mass difference from continuum data ($\Delta M_1 \approx 35$ MeV/c² and $\Delta M_2 \approx 27$ MeV/c².) We observe 42 ± 14 signal events in the $D^{*0}K^+$ mode and 9 ± 6 events in the $D^{*+}K_S^0$ mode.

However, when the $D^{*0}K^+$ candidates are further subdivided into the $D^0 \rightarrow K^-\pi^+$ and $K^-\pi^+\pi^0$ decay channels there is a discrepancy in the D_{s1}^+ yields. As shown in Figure 3, we observe 10 ± 8 signal events in the ΔM_1 distribution for the $D^0 \rightarrow K^-\pi^+$ channel and 33 ± 12 D_{s1}^+ signal events for the $D^0 \rightarrow K^-\pi^+\pi^0$ channel. After accounting for branching fractions and efficiencies, discussed below, this results in a 2.2σ discrepancy in the $D^{*0}K^+$ rates between the two D^0 modes. We cannot rule out the fact that background sources may be contributing a false D_{s1}^+ signal in the $D^0 \rightarrow K^-\pi^+\pi^0$ channel, but not in the $D^0 \rightarrow K^-\pi^+$ channel. However, no such mechanism has been uncovered. To be conservative, we choose to quote only an upper limit for the decay $B \rightarrow D_{s1}^+X$.

Since the D_{s1}^+ reconstruction efficiency increases rapidly with x_p and the D_{s1}^+ momentum distribution from B decays is not known, we compute the inclusive $B \rightarrow D_{s1}^+X$ branching fraction by dividing the data into four equal regions of x_p from 0.05 to 0.45 and summing the efficiency corrected yields. The $D_{s1}^+ \rightarrow D^{*0}K^+$ and $D^{*+}K^0$ branching fractions are equal according to isospin, and their ratio has been measured to be within 30% of unity [14]. We measure the branching fraction $B \rightarrow D_{s1}^+X$ to be $(0.77 \pm 0.22)\%$ from the $D^{*0}K^+$ mode and $(0.28 \pm 0.37)\%$ from the $D^{*+}K_S^0$ mode, where the error is statistical only. The two measurements are statistically consistent. The x_p distribution for our D_{s1}^+ candidates is shown in Figure 4.

IV. CROSS-CHECKS

Several cross-checks, shown in Figure 5, were performed to corroborate the validity of the D_{s1}^+ signal. The scaled continuum background from data after satisfying all selection cuts is negligible, and there is no excess in the ΔM_1 signal region (3 ± 5 events). The uncertainty in the continuum D_{s1}^+ contribution is included in the systematic error. There is also no evidence of peaking in the ΔM_1 signal region for wrong-sign $D^{*0}K^-$ combinations (0 ± 9 events), D^0 mass sidebands (5 ± 5 events), and D^{*0} mass sidebands (-4 ± 6 events).

We have also searched for the D^0 signal from $D_{s1}^+ \rightarrow D^{*0}K^+$ candidates in the ΔM_1 signal region, $|\Delta M_1 - 35 \text{ MeV}/c^2| < 10 \text{ MeV}/c^2$, by relaxing the D^0 mass cut and histogramming the invariant mass of all $K^-\pi^+$ and $K^-\pi^+\pi^0$ combinations that satisfy the remaining selection criteria. In events with multiple candidates per D^0 decay mode we select the candidate with the highest χ^2 probability, which is derived from the reconstructed π^0 and D_{s1}^+ masses. We observe 100 ± 15 D^0 events. However, there are also real D^0 's in the random $D^{*0}K^+$ combinations under the D_{s1}^+ peak; after a ΔM_1 sideband subtraction the D^0 invariant mass spectrum yields 44 ± 18 events (see Figure 6(a)). This is consistent with our $D_{s1}^+ \rightarrow D^{*0}K^+$ yield in Figure 2.

Similarly, we have studied the D^{*0} signal from $D_{s1}^+ \rightarrow D^{*0}K^+$ candidates in the ΔM_1 signal region. We observe 59 ± 15 D^0 events. As in the D^0 case there are also real D^{*0} 's in the random $D^{*0}K^+$ combinations under the D_{s1}^+ peak. After a ΔM_1 sideband subtraction the D^{*0} mass difference spectrum yields 25 ± 18 events (See Figure 6(b)), consistent with our $D_{s1}^+ \rightarrow D^{*0}K^+$ yield.

Finally, we have studied the D_{s1}^+ production from continuum $e^+e^- \rightarrow c\bar{c}$ events. The selection criteria is similar to that used to find D_{s1}^+ from B decays, but since continuum charm production has a hard fragmentation, we require $x_p > 0.5$. In addition, we remove

the $R_2 < 0.3$ cut, relax the charged kaon identification to $\mathcal{R}_K > 0.1$, and remove the Dalitz cut for $D^0 \rightarrow K^-\pi^+\pi^0$. The mass difference distribution for $D^{*0}K^+$ and $D^{*+}K_S^0$ combinations are shown in Figure 7, where the $D^0 \rightarrow K^-\pi^+$ and $K^-\pi^+\pi^0$ modes have been added together. We extract the D_{s1}^+ signal by fitting the data with a Gaussian signal and a threshold background function. The Gaussian width is fixed to the value predicted by Monte Carlo (2.1 MeV/c²), and the mean is allowed to float. We observe 222 ± 19 events in the $D_{s1}^+ \rightarrow D^{*0}K^+$ mode with a mass difference of 35.0 ± 0.2 MeV/c² (statistical error only), and 101 ± 11 events in the $D_{s1}^+ \rightarrow D^{*+}K_S^0$ mode with a mass difference of 27.5 ± 0.3 MeV/c². The results are consistent with the previous CLEO analysis [14].

V. SYSTEMATIC ERRORS AND FINAL RESULTS

There are several sources of systematic error. We assign a systematic error of 16% to account for the 2.2σ discrepancy between the $D^{*0}K^+$ rates for the $D^0 \rightarrow K^-\pi^+$ and $K^-\pi^+\pi^0$ modes. This accommodates different methods of computing the weighted average of the $B \rightarrow D_{s1}^+X$ branching fraction from the four separate decay chains. Uncertainties due to reconstruction efficiencies include 1.5% per charged track, 5% per π^0 , 5% for slow pions from D^* , and 5% for K_S^0 . We also include systematic errors of 7% for Monte Carlo statistics, 5% for kaon identification and the Dalitz decay cut efficiency, 4% for uncertainties in the yield for $x_p < 0.05$, and 8% for uncertainties in the continuum D_{s1}^+ contribution that passes our selection criteria. The total systematic error is 24%.

Averaging the $D^{*0}K^+$ and $D^{*+}K_S^0$ modes together, we obtain $\mathcal{B}(B \rightarrow D_{s1}^+X) = (0.64 \pm 0.19 \pm 0.15)\%$. Since the D_{s1}^+ signal is observed largely in only one decay mode $D_{s1}^+ \rightarrow D^{*0}K^+$ with $D^0 \rightarrow K^-\pi^+\pi^0$, and since there is a discrepancy between this mode and the corresponding mode involving $D^0 \rightarrow K^-\pi^+$, we instead prefer to quote an upper limit on the branching fraction to be $\mathcal{B} < 0.95\%$ at the 90% C.L. [15] This decay rate limit is small relative to the total rate expected for $B \rightarrow \bar{D}^{(*)}D^{(*)}KX$ of about $(7.9 \pm 2.2)\%$ from the wrong-sign D meson yield in B decays [6]. This is not surprising considering the $c\bar{s}$ system has appreciable phase space beyond the D_{s1}^+ mass [4]. Also, CLEO's [16] recent observation of exclusive $B \rightarrow \bar{D}^{(*)}D^{(*)}K$ decays shows that the $D^{(*)}K$ invariant mass distribution lies mostly above the D_{s1}^+ mass.

VI. D_{s1}^+ DECAY CONSTANT

Measurement of the $B \rightarrow D_{s1}^+X$ decay rate also provides an estimate of the D_{s1}^+ decay constant, $f_{D_{s1}^+}$, assuming that the D_{s1}^+ comes dominantly from upper-vertex decays. The inclusive decay rate for B mesons into ground state or excited D_s^+ mesons can be calculated assuming factorization [17],

$$\Gamma(B \rightarrow D_s X) = \frac{G_F^2 |V_{cb}V_{cs}|^2}{16\pi} M_b^3 a_1^2 f_{D_s}^2 I(x, y)$$

where a_1 is the BSW [18] parameter for the effective charged current, and $I(x, y)$ is a kinematic factor with $x = M_{D_s}^2/M_b^2$ and $y = M_c^2/M_b^2$. For scalar or pseudoscalar D_s mesons,

$I(x, y) = \sqrt{(1-x-y)^2 - 4xy(1-x-2y-xy+y^2)}$, and for vector or axial-vector D_s mesons,
 $I(x, y) = \sqrt{(1-x-y)^2 - 4xy(1+x-2x^2-2y+xy+y^2)}$.

We have tightened the x_p requirement to $x_p < 0.35$ since this is the kinematic limit for upper-vertex $B \rightarrow D_{s1}^+ \bar{D}X$ decays. The production of ground state and excited D_s^+ mesons from lower-vertex decays such as $\bar{B} \rightarrow D_{s1}^+ \bar{K}X$ is expected to be suppressed. This is certainly true for $B \rightarrow D_s^+ X$ decays where the fraction of D_s^+ produced at the lower-vertex is measured to be $0.172 \pm 0.079 \pm 0.026$ [19]. Moreover, there is no evidence of D_{s1}^+ production in the region $x_p = 0.35 - 0.45$ where lower-vertex production is likely to occur (see Figure 4.)

With the assumption $f_{D_s^+} = f_{D_s^{*+}}$ we can extract $f_{D_{s1}^+}$ from the ratio of inclusive rates,

$$\frac{\mathcal{B}(B \rightarrow D_{s1}^+ X)}{\mathcal{B}(B \rightarrow D_s^+ X)} = \frac{\Gamma(B \rightarrow D_{s1}^+ X)}{\Gamma(B \rightarrow D_s^+ X) + \Gamma(B \rightarrow D_s^{*+} X)} \approx 0.49 \left(\frac{f_{D_{s1}^+}}{f_{D_s^+}} \right)^2$$

Many systematic errors cancel in the ratio. When computing the D_{s1}^+ decay constant from the above equation, we use $(75 \pm 25)\%$ of the measured $B \rightarrow D_{s1}^+ X$ branching fraction to account for uncertainties in the upper and lower vertex contributions to D_{s1}^+ . This accomodates the excess of $B \rightarrow D_{s1}^+ X$ candidates observed at low $x_p < 0.15$ as seen in Figure 4. From our upper limit on $B \rightarrow D_{s1}^+ X$ and CLEO's [20] measurement of $\mathcal{B}(B \rightarrow D_s^+ X) = (12.11 \pm 0.39 \pm 0.88 \pm 1.38)\%$, we derive $f_{D_{s1}^+}/f_{D_s^+} < 0.40$ at the 90% C.L. The central value is $f_{D_{s1}^+}/f_{D_s^+} = 0.29 \pm 0.06 \pm 0.06$, where the first error is due to the total error in the inclusive $B \rightarrow D_s^+ X$ and $B \rightarrow D_{s1}^+ X$ branching fractions, and the second is the uncertainty in the non-factorizable and lower-vertex contributions to the $B \rightarrow D_{s1}^+ X$ decay rate. Using the measured value of $f_{D_s^+} = 280 \pm 40$ MeV [20] gives $f_{D_{s1}^+} = 81 \pm 26$ MeV which corresponds to an upper limit of $f_{D_{s1}^+} < 114$ MeV. This limit accomodates the prediction of $f_{D_{s1}^+} = 87 \pm 19$ MeV by Veseli and Dunietz [21].

VII. CONCLUSIONS

In summary, we have searched for B mesons decaying into the P-wave $D_{s1}^+(2536)$ meson. The upper limit of $\mathcal{B}(B \rightarrow D_{s1}^+ X) < 0.95\%$ at the 90% C.L. accounts for at most only a fraction of the total wrong-sign $B \rightarrow DX$ rate. Assuming factorization, the decay constant $f_{D_{s1}^+}$ is at least a factor of 2.5 times smaller than the decay constant for the pseudoscalar D_s^+ .

ACKNOWLEDGEMENTS

We gratefully acknowledge the effort of the CESR staff in providing us with excellent luminosity and running conditions. J.P.A., J.R.P., and I.P.J.S. thank the NYI program of the NSF, M.S. thanks the PFF program of the NSF, G.E. thanks the Heisenberg Foundation, K.K.G., M.S., H.N.N., T.S., and H.Y. thank the OJI program of DOE, J.R.P., K.H., M.S. and V.S. thank the A.P. Sloan Foundation, R.W. thanks the Alexander von Humboldt Stiftung, M.S. thanks Research Corporation, and S.D. thanks the Swiss National Science Foundation for support. This work was supported by the National Science Foundation, the U.S. Department of Energy, and the Natural Sciences and Engineering Research Council of Canada.

REFERENCES

- [1] Particle Data Group, R.M. Barnett *et al.*, Phys. Rev. D **54**, 1 (1996).
- [2] I. Bigi, B. Blok, M. Shifman and A. Vainshtein, Phys. Lett. B **323**, 408 (1994).
- [3] A.F. Falk, M.B. Wise, and I. Dunietz, Phys. Rev. D **51**, 1183 (1995); E. Bagan, P. Ball, V.M. Braun, and P. Gosdzinsky, Phys. Lett. B **324**, 362 (1995); M.B. Voloshin, Phys. Rev. D **51**, 3948 (1995).
- [4] G. Buchalla, I. Dunietz, and H. Yamamoto, Phys. Lett. B **364**, 188 (1995).
- [5] B. Blok, M. Shifman, and N. Uraltsev, preprint CERN-TH/96-252.
- [6] CLEO Collaboration, T.E. Coan *et al.*, preprint CLNS 97/1516, CLEO 97-23.
- [7] ALEPH Collaboration, PA05-060, contributed to the 1996 International Conference on High Energy Physics, Warsaw, Poland.
- [8] DELPHI Collaboration, PA01-108, contributed to the 1996 International Conference on High Energy Physics, Warsaw, Poland.
- [9] S. Okubo, Phys. Lett. B **5**, 165 (1963); G. Zweig, CERN Report 8419/TH412 (1964); I. Iizuka, Prog. Theor. Phys. Suppl. **37**, 21 (1966).
- [10] CLEO Collaboration, Y. Kubota *et al.*, Nucl. Inst. and Meth. **A320**, 66 (1992).
- [11] G. Fox and S. Wolfram, Phys. Rev. Lett. **41**, 1581 (1978).
- [12] E691 Collaboration, J.C. Anjos *et al.*, Phys. Rev. D **48**, 56 (1993).
- [13] R. Brun *et al.*, GEANT 3.15, CERN DD/EE/84-1.
- [14] CLEO Collaboration, J. Alexander *et al.*, Phys. Lett. B **303**, 377 (1993).
- [15] The 90% upper limit is derived, assuming Gaussian statistics, by adding 1.28 times the total error to the central value.
- [16] CLEO Collaboration, M. Bishai *et al.*, CLEO-CONF 97-26, EPS97-337, contributed to the 1997 International Europhysics Conference on High Energy Physics, Jerusalem, Israel.
- [17] J.H. Kuhn, S. Nussinov, and R. Ruckl, Z. Phys. C **5**, 117 (1980).
- [18] M. Bauer, B. Stech, and M. Wirbel, Z. Phys. C **29**, 637 (1985).
- [19] CLEO Collaboration, X. Fu *et al.*, CLEO CONF-95-11, EPS0169, contributed to the 1995 International Europhysics Conference on High Energy Physics, Brussels, Belgium.
- [20] CLEO Collaboration, D. Gibaut *et al.*, Phys. Rev. D **53**, 4734 (1996).
- [21] S. Veseli and I. Dunietz, Phys. Rev. D **54**, 6803 (1996).

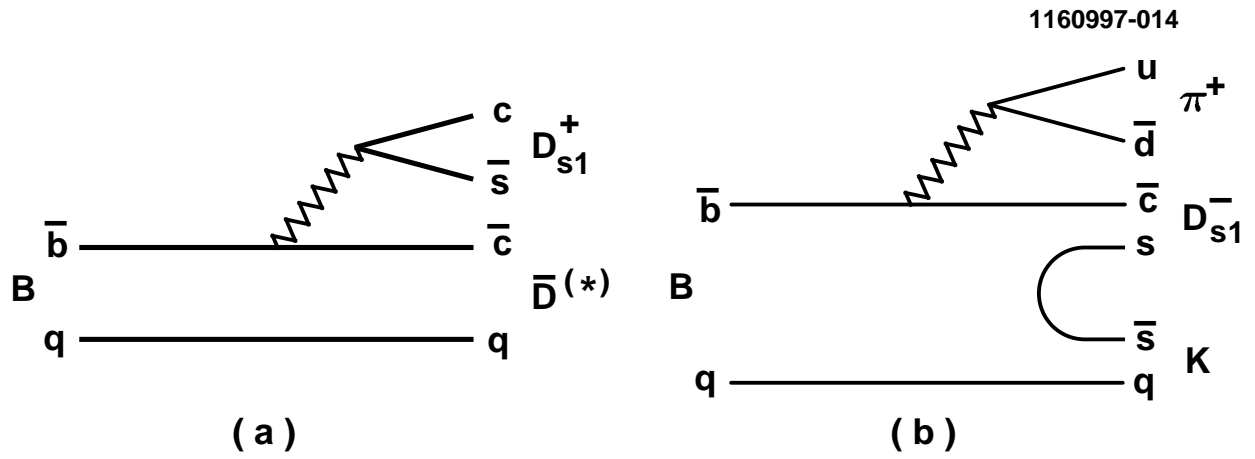


FIG. 1. Feynman diagrams for (a) $B \rightarrow D_{s1}^+ X$ decays producing D_{s1}^+ at the upper-vertex and (b) $B \rightarrow D_{s1}^- X$ decays producing D_{s1}^- at the lower-vertex.

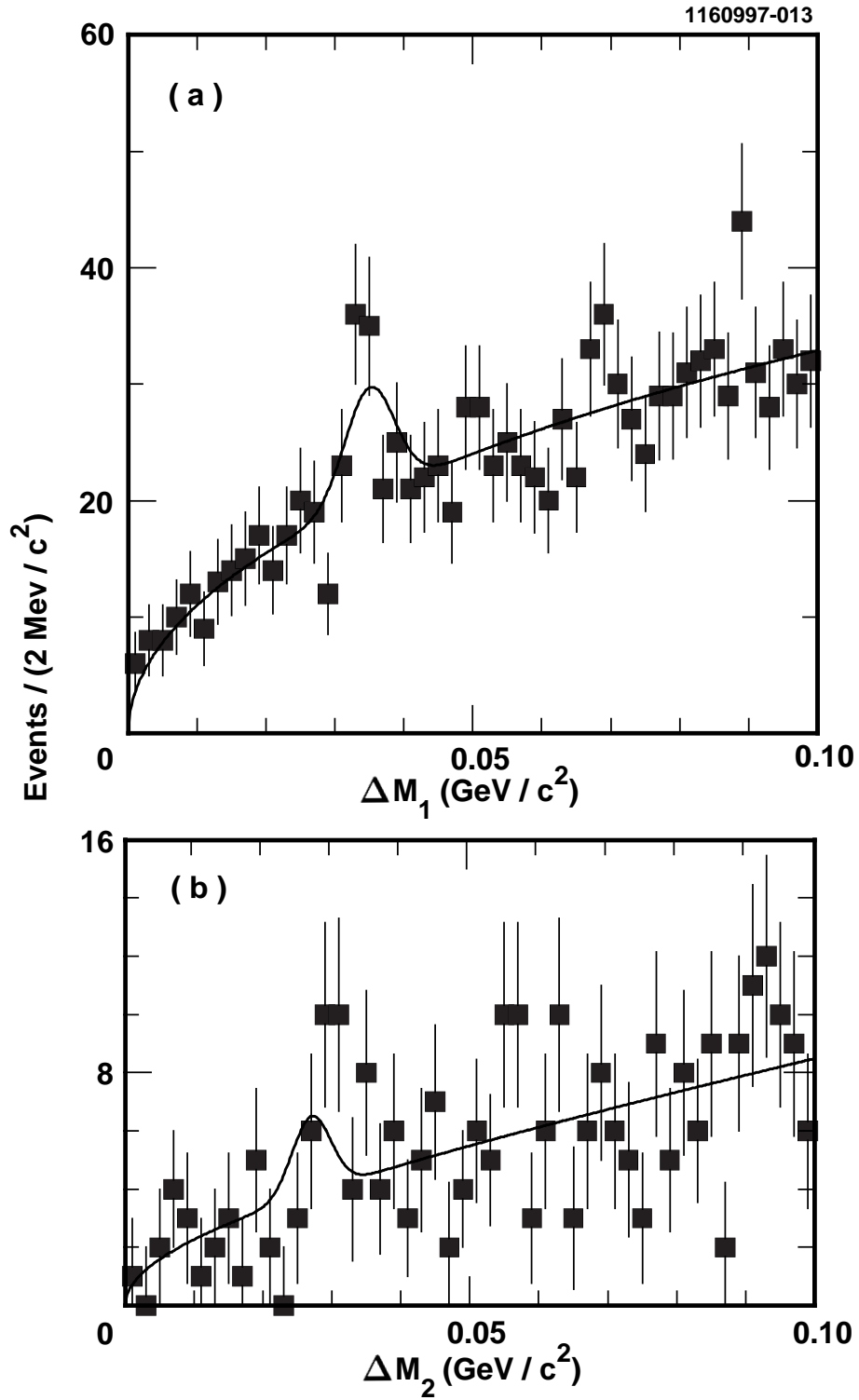


FIG. 2. The mass difference distribution for (a) $D^{*0}K^+$ and (b) $D^{*+}K_S^0$ candidates from B meson decays.

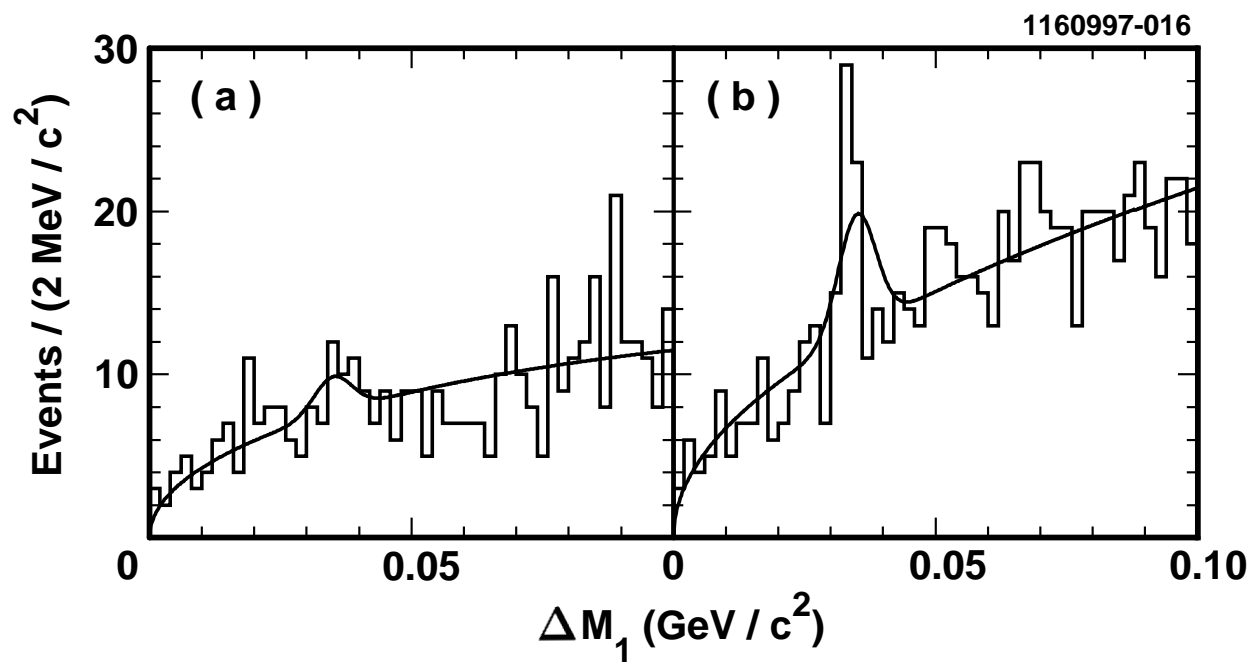


FIG. 3. The ΔM_1 mass difference distribution for $D^{*0}K^+$ candidates from the (a) $D^0 \rightarrow K^-\pi^+$ and (b) $D^0 \rightarrow K^-\pi^+\pi^0$ decay channels.

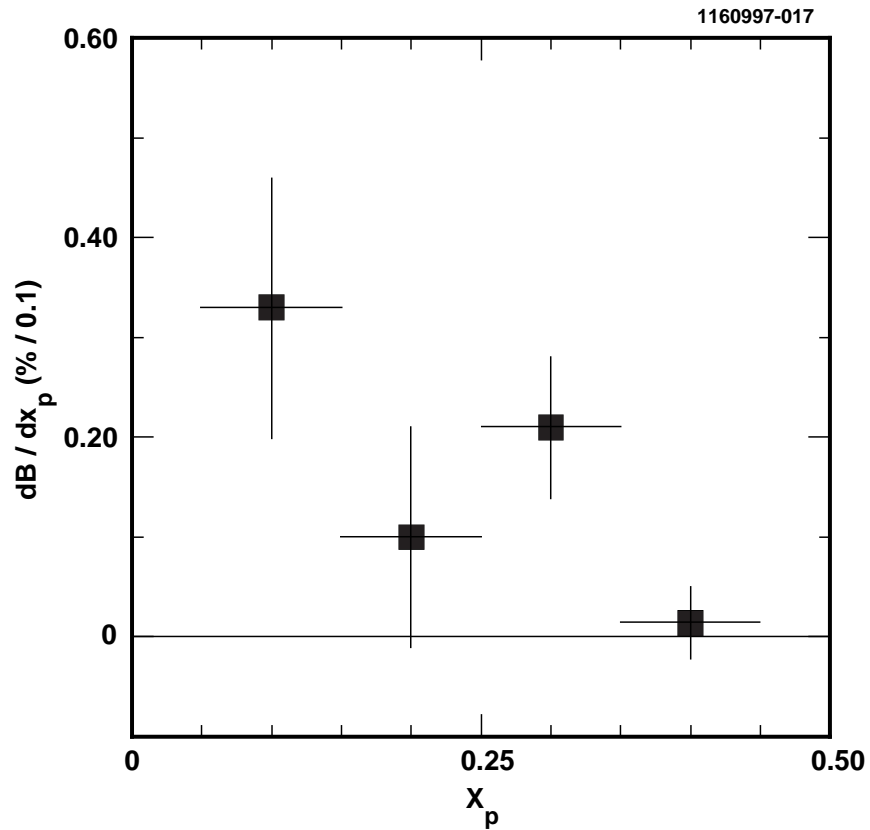


FIG. 4. The efficiency corrected yield for our $B \rightarrow D_{s1}^+ X$ candidates as a function of the D_{s1}^+ scaled momentum x_p . The kinematic limit from upper-vertex and lower-vertex $B \rightarrow D_{s1}^+ X$ decays is $x_p < 0.35$ and $x_p < 0.45$, respectively.

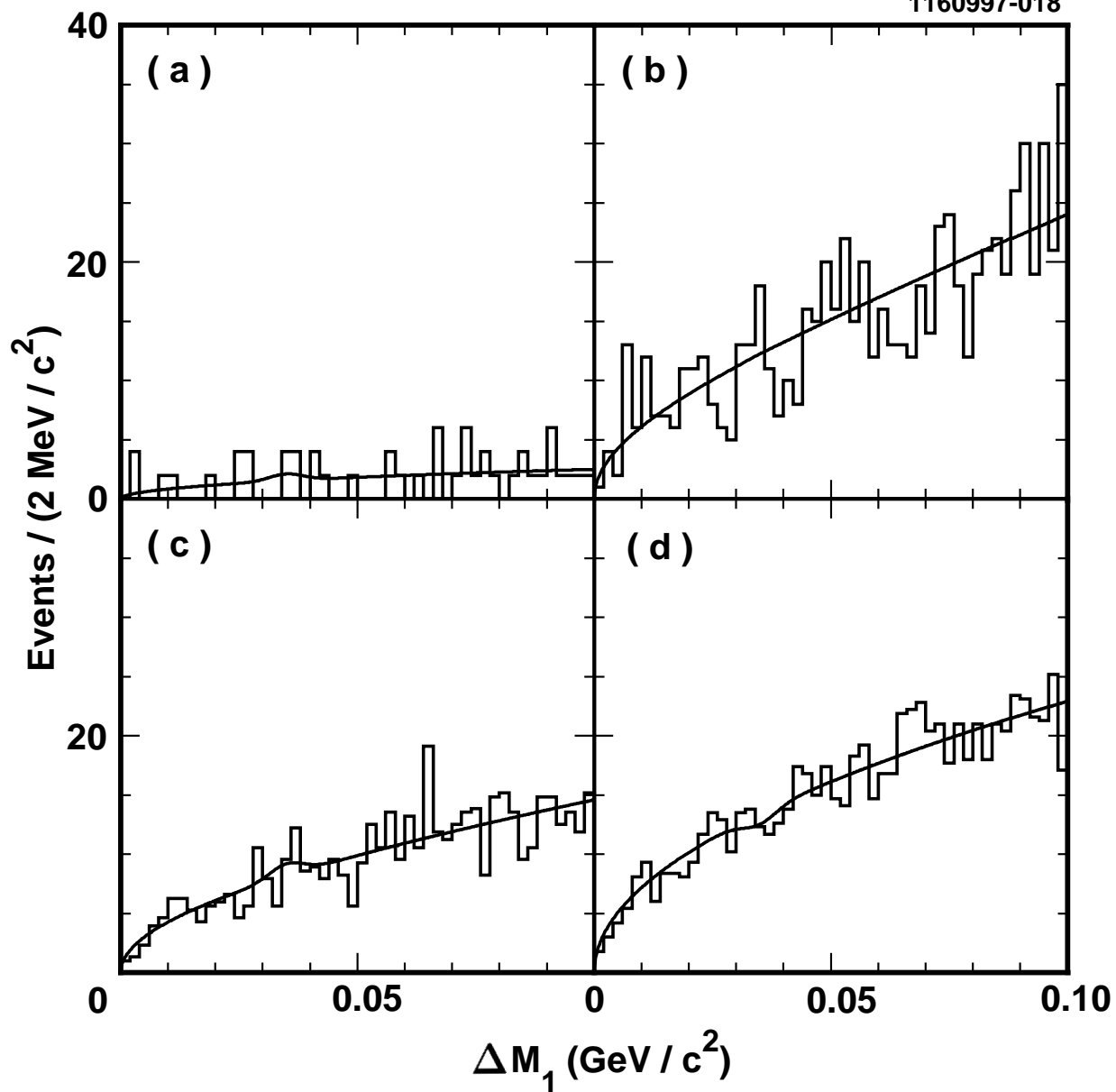


FIG. 5. The normalized $D^{*0}K^+$ mass difference distributions from (a) continuum events, (b) $D^{*0}K^-$ “wrong-sign” combinations, (c) D^0 mass sidebands, and (d) D^{*0} mass sidebands.

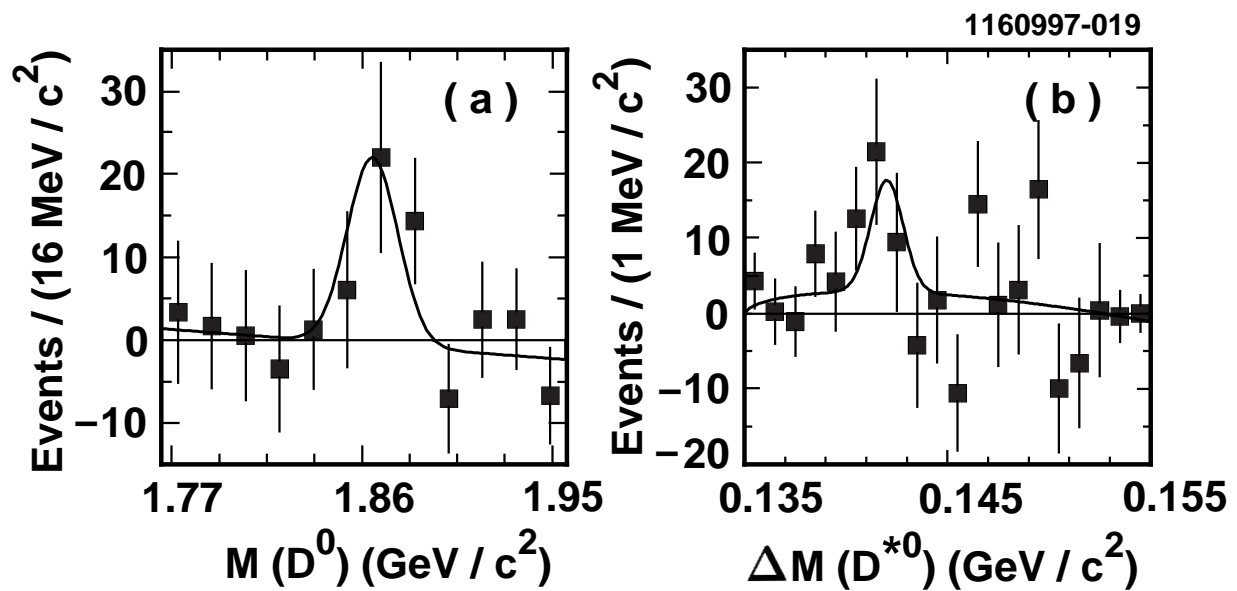


FIG. 6. (a) The invariant mass distribution for $K^-\pi^+$ and $K^-\pi^+\pi^0$ combinations from $D^{*0}K^+$ candidates in the ΔM_1 signal region, after sideband subtraction. (b) The D^{*0} mass difference distribution from $D^{*0}K^+$ candidates in the ΔM_1 signal region, after sideband subtraction.

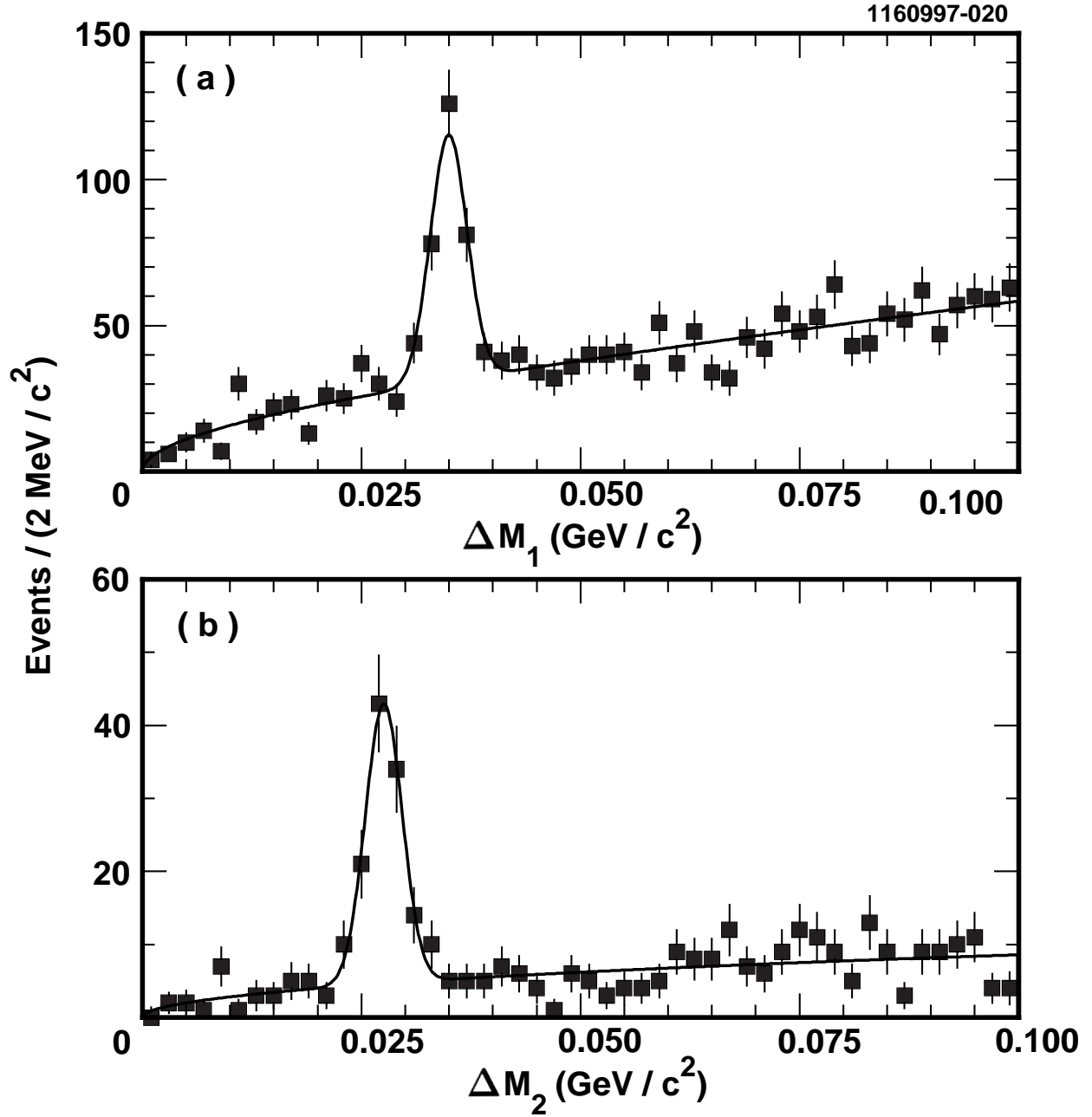


FIG. 7. The mass difference distribution for (a) $D^{*0}K^+$ and (b) $D^{*+}K_S^0$ candidates from continuum $e^+e^- \rightarrow c\bar{c}$ events.